JAMES | Journal of Advances in Modeling Earth Systems

RESEARCH ARTICLE
10.1029/2022MS003084

The Impact of Incremental Analysis Update on Regional Simulations for Typhoons

Yangjinxi Ge[1,2], Lili Lei[1,2,3], Jeffrey S. Whitaker[4], and Zhe-Min Tan[1,2]

[1]Key Laboratory of Mesoscale Severe Weather, Ministry of Education, Nanjing University, Nanjing, China, [2]School of Atmospheric Sciences, Nanjing University, Nanjing, China, [3]Frontiers Science Center for Critical Earth Material Cycling, Nanjing University, Nanjing, China, [4]NOAA Earth System Research Laboratories/Physical Sciences Laboratory, Boulder, CO, USA

Key Points:

- The application of incremental analysis update (IAU) improves 6-hr forecasts and obtains better tropical cyclone (TC) intensity and structure than no initialization
- For regional simulations, three-dimensional IAU with time-constant increments and stronger filtering has advantages over four-dimensional IAU (4DIAU) with time-varying increments
- Due to TC position errors, 4DIAU with 3-hr increment is preferred for TCs as a trade-off between the filtering and time-varying increments

Correspondence to:
L. Lei,
lililei@nju.edu.cn

Citation:
Ge, Y., Lei, L., Whitaker, J. S., & Tan, Z.-M. (2022). The impact of incremental analysis update on regional simulations for typhoons. *Journal of Advances in Modeling Earth Systems*, *14*, e2022MS003084. https://doi.org/10.1029/2022MS003084

Received 14 MAR 2022
Accepted 10 SEP 2022

Abstract The analyses produced by intermittent data assimilation methods can be dynamically inconsistent and unbalanced. By gradually distributing the analysis increment along model integration, the incremental analysis update (IAU) is effective to combat the inconsistences and imbalances. Different implementations of IAU with time constant or time-varying increments using different increment frequencies are systematically evaluated for regional simulations, especially for fast-moving typhoons. Results show that experiments with IAU generally produce smaller forecast errors of temperature, specific humidity, and wind speed than experiment CTRL without initialization. Three-dimensional IAUs (3DIAUs) with time-constant increments have smaller errors than four-dimensional IAUs (4DIAUs) with time-varying increments interpolated from 3-hr and hourly increments. Thus, for regional simulations, 3DIAU that imposes stronger filtering has advantages over 4DIAUs with different increment frequencies. For two typhoon cases, experiments with IAU obtain better intensity and structure of vortex than experiment CTRL; thus, the application of IAU can better retain the observation information and build the improved TC structure. But due to the displacement errors in priors and posteriors, the advantage of 4DIAU that considers the propagation of increment is limited compared to 3DIAU. As a trade-off between the filtering and time-varying increment, 4DIAU with 3-hr increment that considers time-varying increments compared to 3DIAU but imposes stronger filtering than 4DIAU with hourly increment could be preferred for TCs.

Plain Language Summary Data assimilation (DA) provides the best estimate of current state by combining prior information and observations. Most widely used DA methods are intermittent approaches, by which the analyses can be dynamically inconsistent. The insertion noises and imbalances caused by intermittent DA would exacerbate spurious gravity waves and degrade subsequent forecasts. The incremental analysis update (IAU) is an effective way to combat the inconsistences and imbalances by gradually distributing the analysis increment into the model. Here, different configurations of IAU are examined in the regional Weather Research and Forecasting model (WRF). The three-dimensional IAU is found to be more beneficial than the four-dimensional one, because the regional model WRF can simulate fine-scale features and prefers more filtering for the unbalanced analysis increments. For fast-moving systems like typhoons, the application of three-dimensional and four-dimensional IAUs leads to the improved simulated vortex intensity and structure due to reduced gravity wave noises and better retention of observational information.

1. Introduction

Ensemble-based data assimilation (DA) methods, such as the ensemble Kalman filter (EnKF; Evensen, 1994) and hybrid ensemble-variational (EnVAR; Hamill & Snyder, 2000) methods, have been widely used for both regional (Liu & Xiao, 2013; Liu et al., 2009; Schwartz et al., 2021; X. Wang et al., 2008; Zhang & Zhang, 2012) and global numerical weather predictions (Buehner et al., 2013; Clayton et al., 2013; Kleist & Ide, 2015a, 2015b; Kuhl et al., 2013; Whitaker & Hamill, 2002). Previous studies have shown that intermittent DA can cause discontinuities/inconsistencies at analysis times that can be diagnosed by large surface pressure tendencies, and the inserted noises or imbalances into the numerical models can degrade subsequent forecasts (e.g., Harms et al., 1992; Hunt et al., 2004; Fujita et al., 2007). These undesired discontinuities/imbalances can often be diagnosed as large magnitudes of surface pressure tendency (Lynch & Huang, 1992) and can cause spurious gravity waves (Lei et al., 2012b).

There have been various strategies proposed to combat the inconsistencies and imbalances resulted from intermittent DA methods. Nudging (Stauffer & Seaman, 1990, 1994) adds an additional tendency term to the model, allowing small corrections gradually applied within an assimilation time window. Normal-mode initialization (Baer & Tribbia, 1977; Machenhauer, 1977) and digital filtering (DFI; Lynch & Huang, 1992; Huang & Lynch, 1993) apply a balancing procedure after the DA step that eliminates the high-frequency noises from the DA analysis. Incremental analysis update (IAU; Bloom et al., 1996) smoothly distributes the analyses increment from a given DA method over a fixed time window. These initialization methods are effective to mitigate the insertion shocks resulted from intermittent DA methods, but they often rely on empirical parameters (Polavarapu et al., 2004). Thus, a "mollified" EnKF is proposed, which creates balanced analyses by using a continuous formulation of the Kalman filter (Bergemann & Reich, 2010). Similarly, a hybrid nudging EnKF applies EnKF gradually in time via nudging-type terms, aiming to reduce the data insertion shocks (Lei, Stauffer, Haupt, et al., 2012; Lei et al., 2012a). An integrated mass-flux adjustment filter is proposed to diminish spurious mass-flux divergency and surface pressure tendency for convective-scale DA (Zeng et al., 2021).

Among the various strategies to combat the inconsistencies and imbalances, IAU is one of the most widely used methods for both atmospheric and oceanic applications (e.g., Benkiran & Greiner, 2008; Carton et al., 2000; Ha et al., 2017; Ourmières et al., 2006; Rienecker et al., 2008; Zhu et al., 2003). Unlike the intermittent DA methods that update the model field at assimilation times without treatment of the insertion shocks, IAU distributes the analysis increment along the model integration in a continuous and gradual way (Bloom et al., 1996). The traditional IAU, a three-dimensional IAU (3DIAU), takes the analysis increment at the middle of a DA window and applies it as a constant forcing for each time step over the DA window. However, 3DIAU does not take into account the propagation of analysis increments within the DA window. To consider the temporal evolution of analysis increment within the DA window, a four-dimensional IAU (4DIAU) is proposed (Lei & Whitaker, 2016; Lorenc et al., 2015). To prevent the instability associated with IAU when the analysis increment has different scales from the model, IAU with nonconstant weights is also proposed (Takacs et al., 2018).

The 4DIAU has been implemented by several operational centers. At Met Office, hourly analysis increments obtained by the four-dimensional hybrid ensemble-variational (4DEnVar) are used to construct time-varying forcing terms that are digested into the model integration (Lorenc et al., 2015). Their results showed that 4DIAU can filter out high-frequency oscillations introduced by the 4DEnVar while keeping realistic moving features of weather systems. At Environmental Canada, 4DIAU is implemented to gradually absorb time-varying analysis increments from the 4DEnVar, which successfully filtered out spurious gravity waves and also retained more mesoscale information relative to the DFI in terms of the kinetic energy (Buehner et al., 2015). At National Centers for Environmental Prediction (NCEP), 4DIAU is applied for both the deterministic 4DEnVAR analysis and EnKF ensembles, which reduces imbalances generated by the 4DEnVAR and EnKF and produces more accurate forecasts than DFI and 3DIAU (Lei & Whitaker, 2016). The filtering properties of EnKF-3DIAU and EnKF-4DIAU as well as the sensitivities to the assimilation frequency are further discussed by He et al. (2020).

However, few studies have focused on the impacts of IAU on regional simulations, especially for fast-evolving systems like tropical cyclones (TCs). For TCs that contain multiscale features, the insertion noises excited by the inconsistent/imbalanced analysis may degrade the assimilation and subsequent forecast. Previous studies have shown that a degradation of the short-time intensity forecast, especially during the rapid intensification (RI) stage of a TC, can be found, which is defined as a "spindown" issue (Hendricks et al., 2011; Lu & Wang, 2019; Tong et al., 2018; Vukicevic and Aksoy, 2013). The "spindown" is often attributed to the imbalances resulted from the analysis increment, which could be mitigated by IAU. Focused on the RI of hurricane (Patricia, 2015), Lu and Wang (2021) showed that 4DIAU has the limitation of predetermined analysis increments, and the variants of 4DIAU that consider online-computed analysis increments or relocated/feature-relative vortex increments have advantages over 4DIAU for TC track and intensity predictions.

To the best knowledge of the authors, the 3DIAU and 4DIAU have not been systematically examined in a regional model like the Weather Research and Forecasting (WRF; Skamarock et al., 2008), neither for fast-evolving systems like TCs. In this study, the 3DIAU and 4DIAU are applied to the regional WRF with different frequencies of analysis increments used to construct the time-varying tendencies. The impacts of 3DIAU and 4DIAU on regional simulations are first systematically examined. The influences of 3DIAU and 4DIAU on track, intensity, and structure of TC forecasts are also systematically examined for typhoons (Hagibis and Lingling, 2019). Moreover, the impact of the frequency of analysis increment on regional simulations and TC forecasts is also explored.

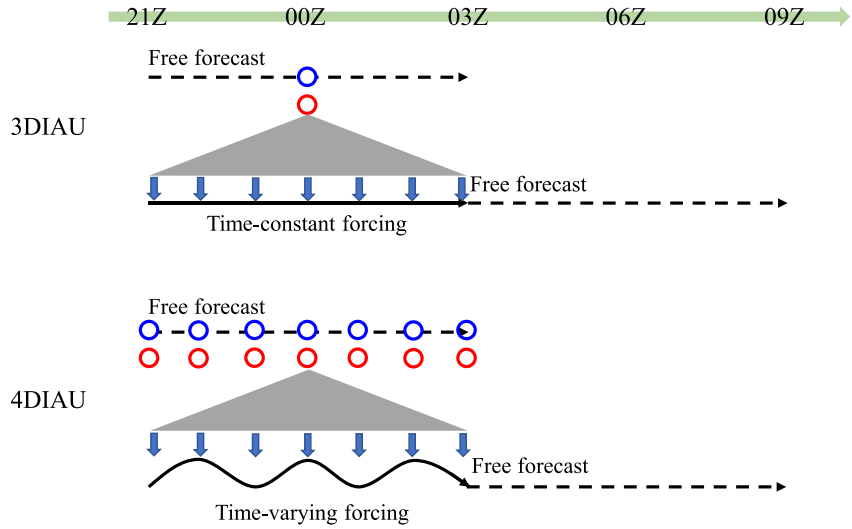

Figure 1. The schematics of three-dimensional incremental analysis update (3DIAU) and four-dimensional incremental analysis update (4DIAU). Blue and red circles denote priors and posteriors, respectively. Blue arrows indicate analysis increment, and black solid lines show time-constant/time-varying incremental analysis update tendencies.

This paper is organized as follows. The schematics of 3DIAU and 4DIAU are briefly described in Section 2. Section 3 presents the details of experimental design, including the model configuration, DA setup, assimilated observations, and verification metrics. Section 4 discusses results of the assimilation experiments for typhoons Hagibis and Lingling. Discussions and conclusions are summarized in Section 5.

2. Methodology

The schematics of 3DIAU and 4DIAU are displayed in Figure 1. Following Lei and Whitaker (2016), a free forecast is advanced from the end of previous assimilation window (2100 UTC) till the end of current assimilation window (0300 UTC), which provides the background/forecast fields $\mathbf{x}_i^f$ (blue circles) where the subscript denotes the time index from -3 to 3. For each analysis time i within a DA cycle, the analysis $\mathbf{x}_i^a$ (red circle) is obtained by updating the background with all observations in the assimilation window through a DA approach. At time i within an assimilation window, the analysis increment is $\Delta\mathbf{x}_i = \mathbf{x}_i^a - \mathbf{x}_i^f$. Instead of inserting the analysis increment to the forecast model at once, IAU allows gradual injection of the increment to the dynamical model by adding an additional forcing term $\mathbf{F}_{IAU}$ into the control model $\frac{d\mathbf{x}}{dt} = f(\mathbf{x}, t)$ as

$$\frac{d\mathbf{x}}{dt} = f(\mathbf{x}, t) + \mathbf{F}_{IAU}. \tag{1}$$

For 3DIAU, the analysis increment at the middle of the assimilation window $\Delta\mathbf{x}_0$ (blue arrow) is equally distributed for each time step within the assimilation window. The time-constant forcing (black solid line) can be written as

$$\mathbf{F}_{3\text{DIAU}} = \frac{\Delta\mathbf{x}_0}{T}, \tag{2}$$

where T is the length of assimilation window (i.e., 6 hr in Figure 1). For 4DIAU, the increments at multiple update times $\Delta\mathbf{x}_i, -3 \le i \le 3$ are linearly interpolated for each time step within the assimilation window. This time-varying forcing (black solid curve) can be given by

$$\mathbf{F}_{4\text{DIAU}}(t) = \frac{\frac{t-t_i}{t_{i+1}-t_i}\Delta\mathbf{x}_{i+1} + \frac{t_{i+1}-t}{t_{i+1}-t_i}\Delta\mathbf{x}_i}{T}, \tag{3}$$

where t_i and t_{i+1} are the closest time indexes for t. A simulation is initialized at the beginning of assimilation window (2100 UTC) with either the time-constant or time-varying forcing till the end of assimilation window

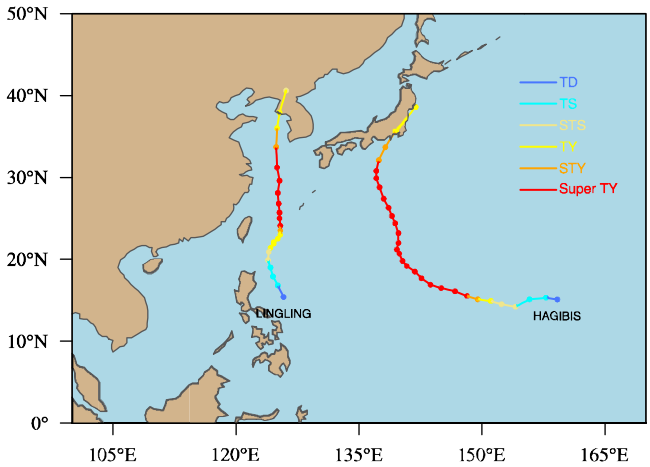

Figure 2. The domain of the assimilation experiments and the observed tracks for typhoons Hagibis and Lingling. Colors of the track denote the typhoon intensity.

(0300 UTC) and is then continuously advanced without IAU forcing to the end of next assimilation window (0900 UTC). The same procedure is repeated for each assimilation cycle.

Compared to 4DIAU that applies time-varying forcing in an assimilation window, 3DIAU uses time-constant forcing and neglects the temporal propagation of increments within an assimilation window. Thus, 3DIAU has stronger filtering impact than 4DIAU as discussed by Lei and Whitaker (2016). Let N be the number of increments used by 4DIAU to construct the time-varying forcing within an assimilation window. When N is 1, 4DIAU degenerates to 3DIAU. When N reaches the maximum, that is, the total time steps in an assimilation window, 4DIAU has no filtering impact.

3. Experimental Design

Experiments are conducted using the WRF (version 3.9; Skamarock et al., 2008) model. The WRF model has a single domain with a 12-km horizontal grid spacing and 560 × 720 grid points. There are 56 vertical levels, and the model top is at 10 hPa. The whole domain coverage is shown in Figure 2. Following C. Wang et al. (2020), the physical parameterization schemes include the single-moment 6-class microphysics scheme (Hong & Lim, 2006), the Yonsei University Scheme planetary boundary layer scheme (Hong et al., 2006), the unified Noah land surface model (Tewari et al., 2004), the Rapid Radiative Transfer Model for GCMs and shortwave and longwave schemes (Iacono et al., 2008), and the Kain Fritsch cumulus parameterization scheme (Kain, 2004).

The assimilated observations are the conventional observations and clear-sky radiance observations from the NCEP Global Data Assimilation System (GDAS) and TC information from the Tropical Cyclone Vitals Database (TCVitals). Conventional observations include all in situ observations and cloud motion vectors (https://www.emc.ncep.noaa.gov/mmb/data_processing/prepbufr.doc/table_2.htm). Radiance observations include the Advanced Microwave Sounding Unit-A, the Atmospheric Infrared Sounder, the Microwave Humidity Sounder, and the High-resolution Infrared Radiation Sounder (https://www.emc.ncep.noaa.gov/mmb/data_processing/prepbufr.doc/table_18.htm). TC information uses the minimum sea level pressure (SLP) along with the latitude and longitude of a TC. The observation priors that are estimated observations from the state variables are computed by the Gridpoint Statistical Interpolation analysis system (Kleist et al., 2009; Wu et al., 2002). The observation error covariances are the same as those used by the NCEP GDAS.

The National Oceanic and Atmospheric Administration operational four-dimensional hybrid ensemble-variational (4DEnVAR) system (Kleist & Ide, 2015a, 2015b) and ensemble square root filter (EnSRF; Whitaker & Hamill, 2002) are used to assimilate the observations every 6 hr. The deterministic analysis is produced by 4DEnVAR, while the 80-member ensemble is updated by EnSRF. No recentering is applied for the ensemble. As an extension of the three-dimensional hybrid ensemble-variational method (3DEnVAR; Hamill & Snyder, 2000; Lorenc, 2003), 4DEnVAR uses multiple time slices of hybrid background error covariances within an assimilation window, which combines the static background error covariances and flow-dependent sample background error covariances estimated from an ensemble forecast. It is demonstrated that 4DEnVAR performs better than 3DEnVAR by considering the variation of observations within the assimilation window and the evolution of background information. Here, the weight for static background error covariances is 0, and thus, the background error covariances are purely from the ensemble (Feng & Wang, 2021). To mitigate sampling errors caused by a limited ensemble size and model errors, the covariance localization and inflation are applied. By using the Gaspari and Cohn (1999) localization function, observations have no impact on the state variables when the horizontal (vertical) distance between an observation and a state variable is larger than 1,000 km (1.5 scale heights). The relaxation to prior spread (Whitaker & Hamill, 2012) method with a relaxation factor of 1.15 is used for covariance inflation.

To analyze the impact of IAU on regional simulations, especially for TCs, four assimilation experiments are conducted, whose analyses are computed by the 4DEnVAR with hourly ensemble backgrounds. Experiment CTRL has no initialization except the assimilation update. Experiment 3DIAU evenly distributes the analysis increment at the middle

of an assimilation window (00Z in Figure 1) over the whole assimilation window. Experiment four-dimensional incremental analysis update with 3-hr analysis increments (4DIAU3H) uses 3-hr analysis increments (21Z, 00Z, and 03Z in Figure 1) to construct the time-varying forcing for an assimilation window. Similarly, experiment 4DIAU uses hourly increments (from 21Z to 03Z in Figure 1) to construct the time-varying forcing, which has a higher temporal resolution than experiment 4DIAU3H. All assimilation experiments are carried out for two TC cases whose observed tracks are shown in Figure 2. One is typhoon Lingling (2019) and the other is typhoon Hagibis (2019). Assimilation experiments are cycled from 0000 UTC 31 August to 1200 UTC 7 September 2019 for the former and from 1200 UTC 3 October to 1200 UTC 12 October 2019 for the latter. For each case, the assimilation experiments are started 2 days before the TC is named, which give 37 assimilation cycles for typhoon Hagibis and 31 assimilation cycles for typhoon Lingling. The first 2 days of assimilation experiments are not used for verification.

To evaluate the performances of 3DIAU and 4DIAU on regional simulations, domain-averaged root-mean-square (RMS) errors of 6-hr priors are calculated in both observation and model spaces. For observation-space verification, RMS errors against conventional observations, including land and marine surface stations, rawinsonde, and aircraft reports, are computed. For model-space verification, RMS errors against the NCEP Final Operational Global Analysis (FNL) with a horizontal resolution of 0.25° are computed. The location, minimum SLP, and maximum wind speed (MWS) of the vortex from the TCVitals are used to evaluate the TC forecasts. Moreover, measurements of the TC structure, like the radius of maximum wind (RMW), four-quadrant radius of gale-force wind (R17), and TC fullness (Guo & Tan, 2017), are also examined.

4. Results

4.1. Verifications in Observation and Model Spaces

To evaluate the IAU performances on regional simulations, 6-hr priors of assimilation experiments are verified against the conventional observations and NCEP FNL analyses, respectively. Error profiles are averaged over the domain and simulation times for both typhoons Hagibis and Lingling, and the error differences of experiments with IAU compared to experiment CTRL are shown in Figures 3 and 4. Negative (positive) values denote smaller (larger) errors than experiment CTRL. The significance of the differences among the assimilation experiments is examined using a paired sample t test for the error samples of experiments at each assimilation cycle. The error differences between the experiment CTRL and experiments with IAU that are significant at the 95% confidence level are shown by the dots. Bars on top denote the mean error differences, and the mean error differences among the assimilation experiments are all significant at the 95% confidence level, except the experiment four-dimensional incremental analysis update with 3-hr analysis increments (4DIAU3H) compared to CTRL for specific humidity in observation space and the experiment 4DIAU3H compared to experiment 4DIAU for temperature in model space.

As shown in Figure 3, experiments with IAU have significantly smaller temperature errors than experiment CTRL for nearly all vertical levels, except for near-surface levels. Experiment 3DIAU has slightly but significantly smaller mean temperature error than experiment 4DIAU3H, and both of them have slightly but significantly smaller mean temperature errors than experiment 4DIAU. For the wind speed, experiment 3DIAU produces significantly smaller errors than experiment CTRL for all vertical levels, except for 400 hPa. Experiment 4DIAU3H has generally smaller wind speed errors than experiment CTRL, except for levels between 500 and 200 hPa. Experiment 4DIAU has larger wind speed errors than experiment CTRL for levels between 900 and 300 hPa. Three experiments with IAU have significantly smaller mean errors of wind speed than experiment CTRL, while experiment 3DIAU has significantly smaller mean errors than 4DIAU3H, and experiment 4DIAU3H has significantly smaller errors than 4DIAU. For the specific humidity, experiment 3DIAU obtains smaller errors than experiment CTRL for model levels below 400 hPa, while experiments 4DIAU and 4DIAU3H have larger errors than experiment CTRL between 900 and 300 hPa. Experiment 4DIAU3H has a similar mean-specific humidity error to experiment CTRL, while experiment 3DIAU (4DIAU) has a significantly smaller (larger) mean-specific humidity error than experiment CTRL.

Results from verifications against the NCEP FNL analyses (Figure 4) are generally consistent with those verified against the conventional observations (Figure 3). Experiments with IAU in general have significantly smaller temperature errors than experiment CTRL for all vertical levels, except for near the surface and 300 hPa. Experiments 4DIAU3H and 4DIAU have similar mean temperature errors, and both have significantly larger mean temperature errors than experiment 3DIAU. Experiments with IAU have significantly smaller wind speed errors

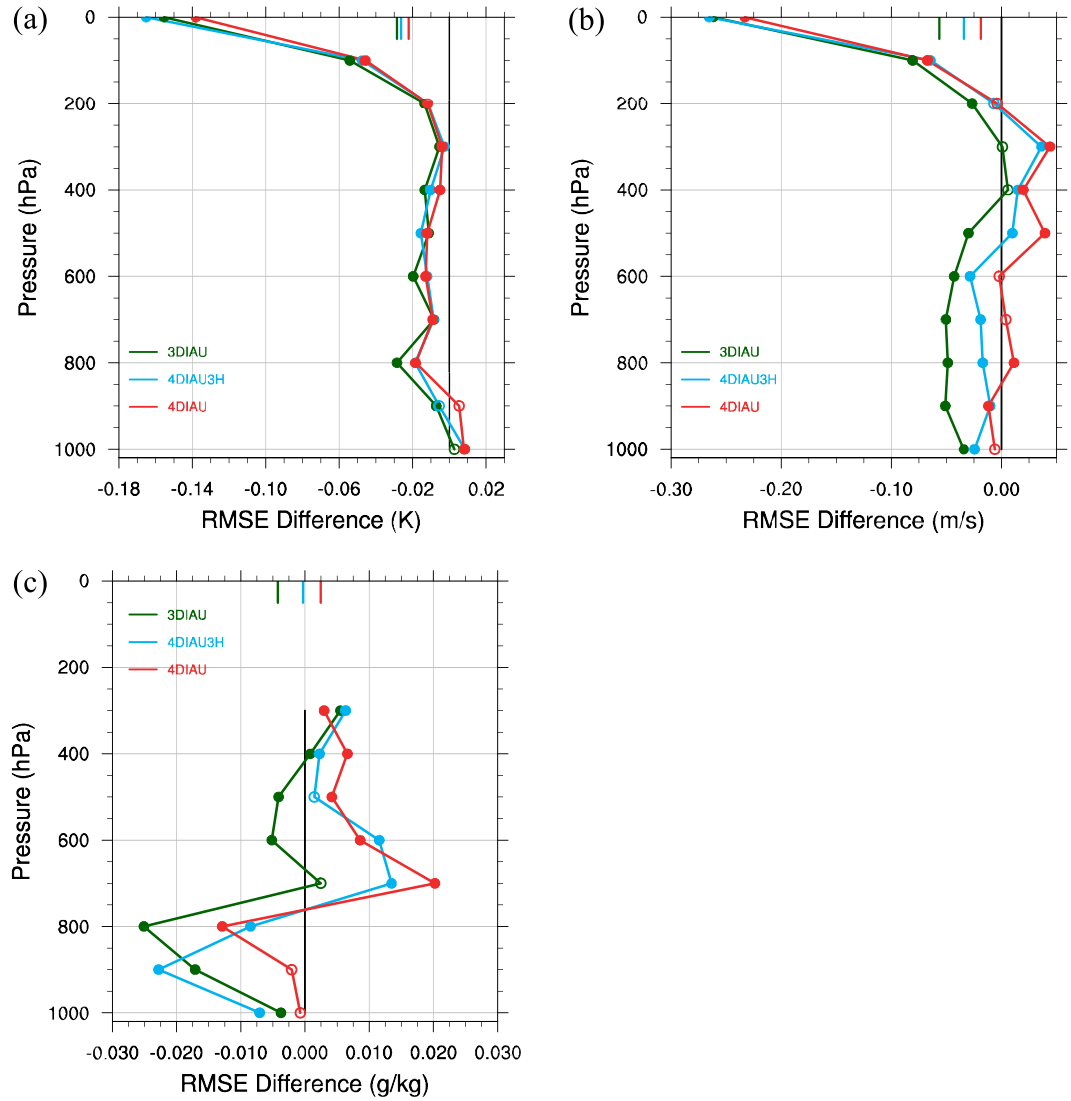

Figure 3. Profiles of 6-hr prior error differences between experiments with incremental analysis update and experiment CTRL for (a) temperature, (b) wind speed, and (c) specific humidity. The errors are verified against the conventional observations and averaged over the domain and simulation times for both typhoons Hagibis and Lingling. Dots indicate that the error differences are statistically significant at the 95% confidence level, and circles indicate insignificant differences. Bars on top denote the mean error differences, and the mean error differences among the assimilation experiments are all significant at the 95% confidence level, except the experiment four-dimensional incremental analysis update with 3-hr analysis increments (4DIAU3H) compared to CTRL for specific humidity.

than experiment CTRL for all vertical levels, except for 200 hPa. Experiment 3DIAU has significantly a smaller mean wind speed error than 4DIAU3H, and experiment 4DIAU3H has significantly smaller mean errors than 4DIAU. Experiment 3DIAU has significantly smaller errors of specific humidity than CTRL for all vertical levels. Experiment 4DIAU3H has smaller errors of specific humidity than CTRL around 850 hPa, and experiment 4DIAU has smaller errors of specific humidity than CTRL above 700 hPa.

There are some discrepancies between the verifications in observation space and model space for different vertical levels, which are possibly due to the inhomogeneous distributions of the conventional observations. The comparisons among experiments CTRL and IAUs are generally consistent. Experiments with IAU have significantly smaller errors of temperature and wind speed than CTRL. For specific humidity, experiment 3DIAU has significantly smaller errors than CTRL, and experiments 4DIAU3H and 4DIAU have similar or significantly larger errors than CTRL. For all variables, experiment 3DIAU has significantly smaller errors than experiments 4DIAU3H and 4DIAU, and experiment 4DIAU3H generally has significantly smaller errors than 4DIAU.

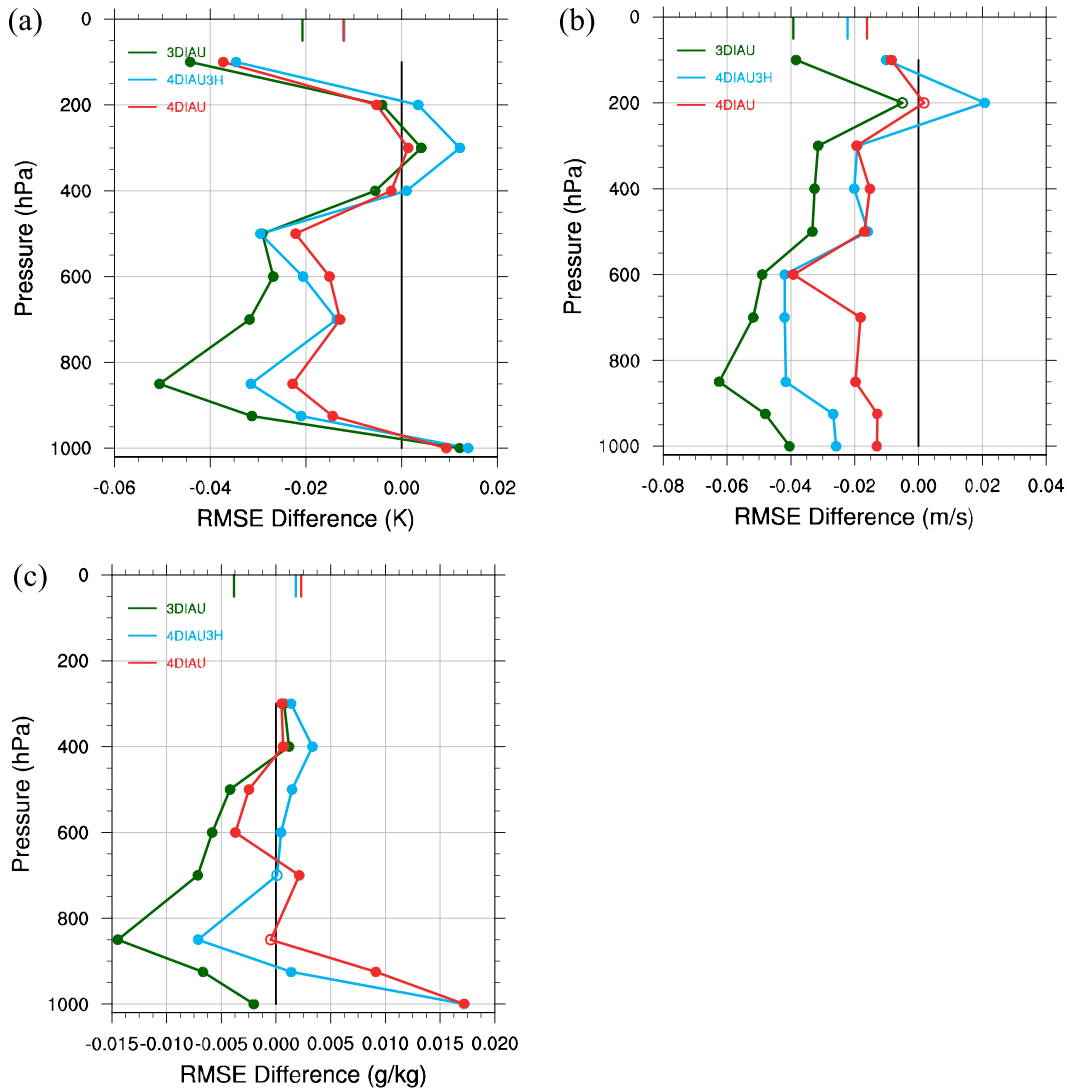

Figure 4. Same as Figure 3, except for (a) temperature, (b) wind speed, and (c) specific humidity verified against the National Centers for Environmental Prediction Final Operational Global analyses. The mean error differences among the assimilation experiments are all significant at the 95% confidence level, except the experiment four-dimensional incremental analysis update with 3-hr analysis increments (4DIAU3H) compared to experiment four-dimensional incremental analysis update for temperature.

Table 1
Spatially and Temporally Averaged Absolute Values of Surface Pressure Tendency (hPa/3h) From Each Assimilation Experiment for Typhoons Hagibis and Lingling

Experiment	Hagibis	Lingling
CTRL	29.16	29.05
3DIAU	6.81	6.65
4DIAU3H	6.83	6.67
4DIAU	6.86	6.71

Note. To clearly show the differences of imbalances among the assimilation experiments, the surface pressure tendency is averaged from instantaneous values with unit scaled from Pa/s to hPa/3h. The differences of the surface pressure tendency among the assimilation experiments are all statistically significant at the 95% confidence level.

Following previous studies (e.g., Lei & Whitaker, 2016; Lei et al., 2012b), the surface pressure tendency is computed for each assimilation experiment to quantitatively analyze the imbalance caused by DA. Table 1 shows the spatially and temporally averaged absolute values of surface pressure tendency for typhoons Hagibis and Lingling. The domain-averaged surface pressure tendency from a regional simulation can be more influenced by position errors of weather systems than that from a global model. But the relative imbalances of experiment CTRL compared to experiments with IAU can still show the effectiveness of IAU on mitigating the imbalance. Experiments with IAU have significantly smaller magnitudes of surface pressure tendency than experiment CTRL. Thus, consistent with previous studies (Bloom et al., 1996; Lei & Whitaker, 2016), the application of IAU helps to reduce the imbalance imposed by DA. Moreover, experiment 3DIAU has significantly smaller magnitudes of surface pressure tendency than 4DIAU3H, and experiment 4DIAU3H has significantly smaller

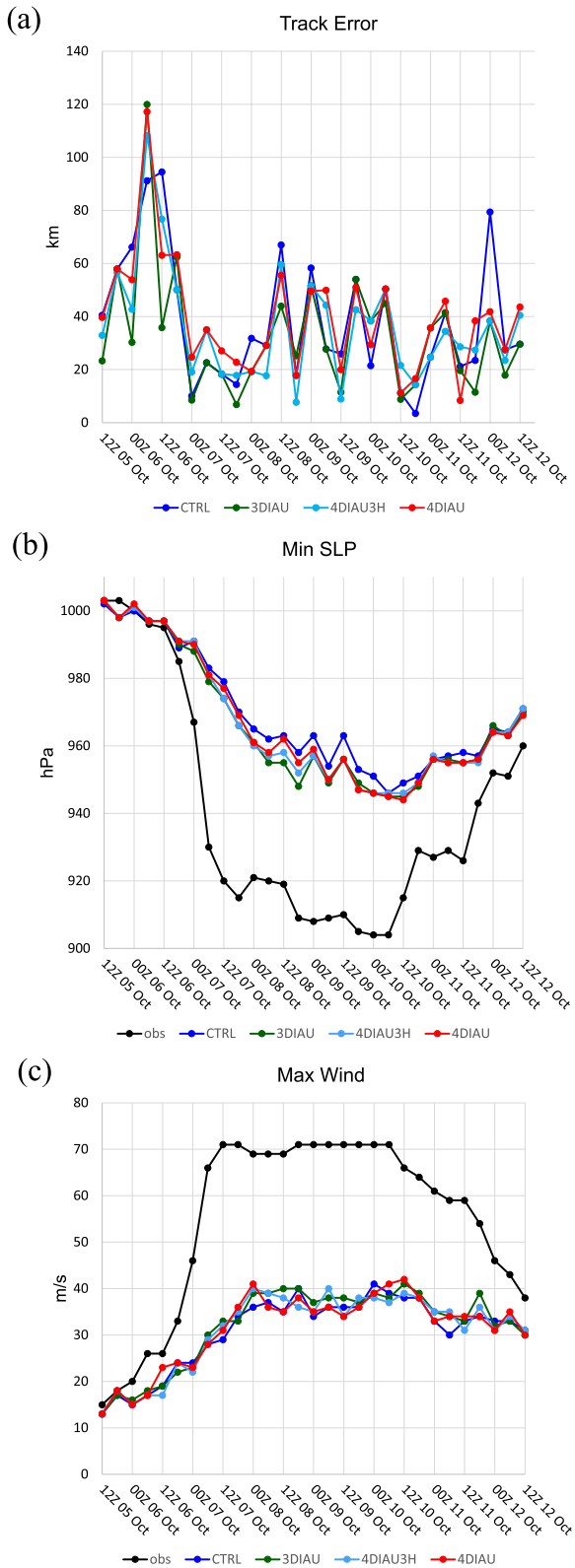

Figure 5. For typhoon Hagibis, (a) track errors of 6-hr priors from assimilation experiments verified against the observed value, and the observations and 6-hr priors for (b) minimum sea level pressure (SLP) and (c) maximal wind speed.

magnitudes of surface pressure tendency than 4DIAU. This is because 3DIAU imposes a stronger filtering impact than 4DIAU and more frequent 4DIAU increments lead to a less filtering impact (Lei & Whitaker, 2016).

The imbalances resulted from DA could cause spurious gravity waves and degrade subsequent forecasts. Thus, these imbalance analyses are consistent with previous verifications of temperature, wind speed, and specific humidity in observation and model spaces (Figures 3 and 4). Experiments with IAU have smaller errors than experiment CTRL, because IAU effectively reduces imbalances caused by DA and helps the model to retain observation information. Experiment 3DIAU has smaller errors than that of 4DIAU3H, and experiment 4DIAU3H has smaller errors than that of 4DIAU, which is led by strong to weak filtering impacts from different implementations of IAU. But Lei and Whitaker (2016) showed that using the NCEP GFS model, EnKF-4DIAU has smaller errors of temperature and wind speed than EnKF-RAW that has no IAU applied (similar to experiment CTRL here), and EnKF-RAW has smaller errors than EnKF-3DIAU. Meanwhile, EnKF-3DIAU has smaller values of surface pressure tendency than EnKF-4DIAU, and EnKF-4DIAU has smaller values of surface pressure tendency than EnKF-RAW. Results of Lei and Whitaker (2016) are inconsistent with results here, which are possibly due to different magnitudes of imbalance in different models. Compared to the global model GFS, the regional model WRF often has higher spatial resolutions for simulations and assimilation updates and also less damping, and thus in WRF, 3DIAU that imposes stronger filtering has advantages over 4DIAU.

4.2. Impacts of IAU on TC Assimilations and Forecasts

Figures 5 and 6 show the track errors of 6-hr priors from assimilation experiments verified against the observed values and the observations and 6-hr priors of minimum SLP and MWS from assimilation experiments, for typhoons Hagibis and Lingling, respectively. Assimilation experiments with and without IAU have similar 6-hr track errors. The 6-hr minimum SLP and MWS of the assimilation experiments are comparable to the observed intensity when the vortexes are weak, but there are large discrepancies when the vortexes are strong (Islam et al., 2015; Ren et al., 2019; Sawada et al., 2019). Compared to experiment CTRL, experiments with IAU have smaller 6-hr minimum SLP errors from the RI till the maximum intensity reached. Similar results are obtained for the MWS, except that the benefits of IAU are reduced.

Besides the track and intensity as commonly used evaluation metrics for TCs, the TC structure, including the RMW, radius of gale-force wind (R17), and fullness (Guo & Tan, 2017) of 6-hr priors, is verified against the observed quantities. The fullness, as a measurement of intensity, favors a larger value (i.e., a stronger vortex), given a smaller RMW and a larger R17 (Guo & Tan, 2017). Consistent with the underestimation of TC intensity as shown by the verifications of minimum SLP and MWS (Figures 5 and 6), the assimilation experiments have larger RMWs, smaller R17s, and smaller values of fullness than the observed quantities (figures are not shown). Averaged over the lifetimes of typhoons Hagibis and Lingling, respectively, normalized TC structure errors of 6-hr priors from experiments with IAU compared to experiment CTRL show that the application of IAU significantly reduces RMW errors than experiment CTRL and generally significantly smaller R17 errors than experiment CTRL (Figure 7). Experiments with IAU have similar errors of RMW and R17. Consequently, for the fullness that is an integrated

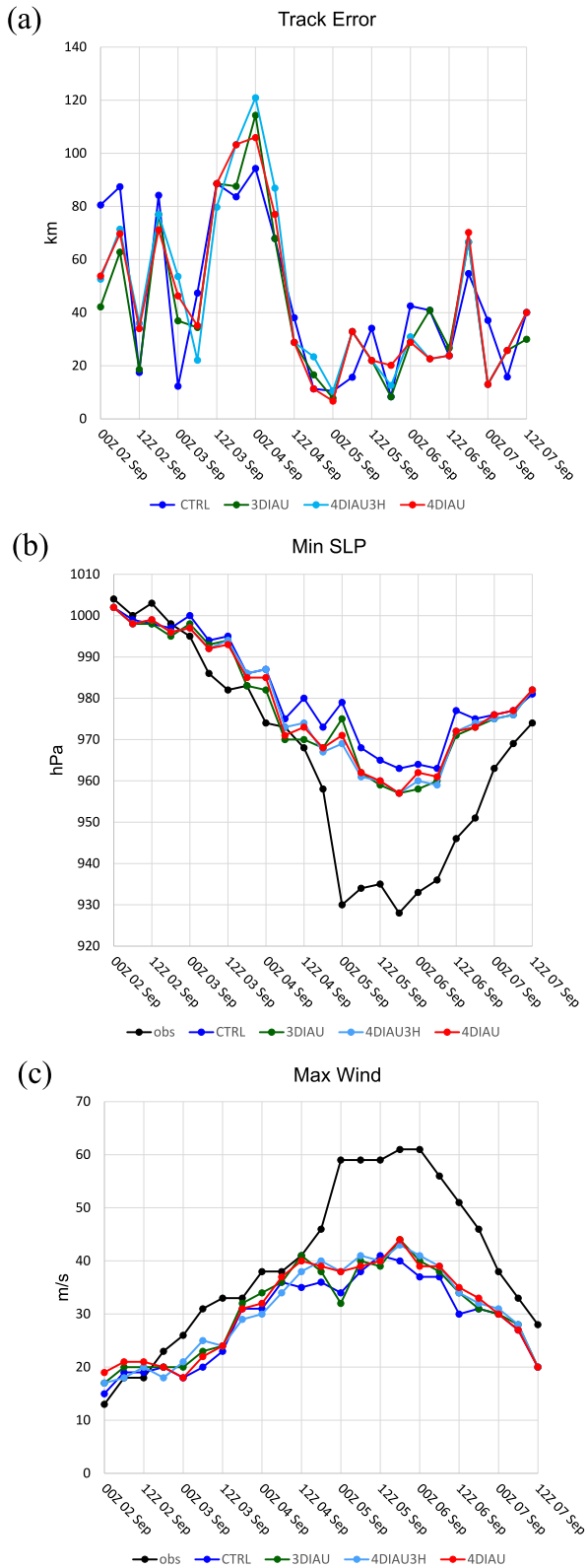

Figure 6. Same as Figure 5, except for typhoon Lingling.

measurement of the TC outer-core and inner-core structures, experiments with IAU have similar errors to each other, and all of them have significantly smaller errors than experiment CTRL with the advantages mainly led by the improvement of RMW. Moreover, experiment CTRL has smaller sample sizes of R17 that measures the TC outer-core size than experiments with IAU during the first few cycles. This is because that experiment CTRL fails to develop the TC structure during the early stage of development (figures are not shown). Thus, besides the benefit of capturing a better vortex size, the application of IAU can help the model to form a more realistic TC during its developing stage.

For both TC cases, 5-day forecasts are launched every 12 hr during the TC lifetimes for each assimilation experiment. The RMS errors of track, minimum SLP, and MWS verified relative to the observed values are shown as a function of forecast lead time (Figure 8). Experiments with IAU have smaller track errors than CTRL at the initial time, and then experiment 4DIAU has gradually faster track error growth than the other experiments. Due to the limited sample size especially with long forecast lead times, it is hard to draw a statistical conclusion for the impact of IAU on track errors. For the minimum SLP, experiments with IAU have smaller errors than CTRL till 24 hr, and afterward, they have similar errors to CTRL. Experiments with IAU have similar MWS errors to CTRL at different lead times. The results are consistent with previous studies that IAU has more prominent impacts on the state variable SLP that is more sensitive to imbalances (He et al., 2020; Lei & Whitaker, 2016).

To further analyze the effect of IAU on a vortex, single-cycle experiments with and without IAU are conducted for the assimilation window centered at 1800 UTC 7 October 2019 at which typhoon Hagibis experienced the RI. The same priors and posteriors from experiment CTRL during the assimilation window are used for IAU experiments with free forecasts till the end of next assimilation window at 0300 UTC 8 October 2019. For single-cycle experiments with and without IAU, the 15-min minimum SLP and MWS at the lowest model level in two adjacent assimilation windows are shown in Figure 9, and the hourly two-dimensional snapshots of the SLP and wind speed at the lowest model level within the first assimilation window are displayed in Figure 10. As shown in Figure 9, experiment CTRL suffers spindown shown by the rapid vortex weakening during the first 1 hr forecast (Lu & Wang, 2019) and then has the vortex gradually reintensified after several hours. Compared to experiment CTRL, experiments with IAU have the minimum SLP and MWS gradually evolving during the assimilation window without the symptom of spindown. Consistently, the intermittent update of SLP and wind field are clearly shown in experiment CTRL, while gradual evolutions of the SLP and wind field are obtained from the experiments with IAU (Figure 10). Note that assimilation experiments with or without IAU have improved TC locations than the free forecast. Experiments with IAU have similar evolutions of minimum SLP and MWS, except that experiment 4DIAU has a weaker vortex than experiments 3DIAU and 4DAIU3H.

To further examine the spindown happened during the first 1 hr forecast of CTRL, 15-min evolutions of SLP and wind speed at the lowest model level from 1800 UTC to 1900 UTC 7 October 2019 (0–1 hr of Figure 9) for experiments with and without IAU are shown in Figure 11. Consistent with Figures 9 and 10, experiment CTRL undergoes a rapid vortex weakening in the first 15 min. The CTRL analysis at 0 hr exhibits a strong vortex with the

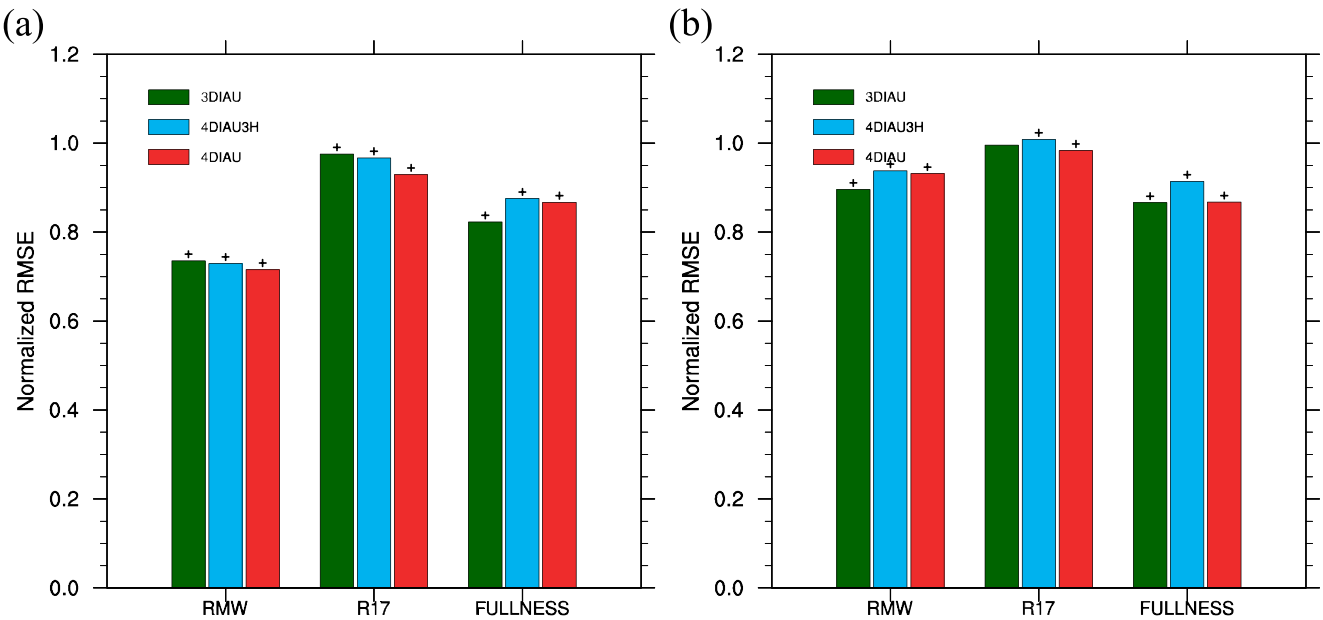

Figure 7. Normalized errors of radius of maximum wind, radius of gale-force wind (R17), and fullness of 6-hr priors from each assimilation experiment compared to experiment CTRL for typhoons (a) Hagibis and (b) Lingling. The plus symbol indicates that the differences between the assimilation experiments and CTRL are statistically significant at 95% confidence level. The differences among the experiments with incremental analysis update are insignificant at 95% confidence level. The value of 1 means that the errors of assimilation experiments are the same as experiment CTRL.

minimum SLP lower than 970 hPa and MWS larger than 32 m/s. But after 15 min, the pressure and wind fields are strongly adjusted, especially the pressure, and the initially strong vortex is rapidly weakened. Comparatively, the pressure and wind fields of experiments with IAU at 0 hr are integrated from −3 hr, which provide a slightly weaker but more balanced vortex than that of CTRL. At 15 min, compared to the sudden adjustment shown in experiment CTRL, experiments with IAU have gradually evolving pressure and wind fields from 0 min, which provide more coherent inner- and outer-core structures. Till 1 hr, experiments with IAU still have stronger winds in the inner core of the vortex, which are better agreed to the observed quantities than experiment CTRL. This is consistent with previous verifications of TC intensity and structure. It has demonstrated that IAU can help the model to better retain the observation information and build the improved TC structure and its evolution.

To investigate the impact of imbalance caused by DA on TC, Figure 12 shows the evolution of dry air mass tendency from 1800 UTC to 2000 UTC 7 October 2019 (0–2 hr of Figure 9) for experiments CTRL and 3DIAU. Dry air mass as a prognostic variable in WRF gives the mass of dry air in a column, which is directly contributed to the surface pressure that is a diagnostic variable in WRF. The tendency is calculated every 15 min and its unit is adjusted to hPa/3h. The evolutions of dry air mass tendency for experiments 4DIAU and 4DIAU3H are similar to experiment 3DIAU (figures are not shown), although the magnitudes of dry air mass tendency for 4DIAU and 4DIAU3H are slightly larger than those for 3DIAU. At 15 min, experiment CTRL has large values of pressure tendency around the TC center, which is consistent with the strong adjustment of pressure and wind fields (Figure 9) and also consistent with the large domain averaged surface pressure tendency (Table 1). These large values of pressure tendency are spread out by the gravity waves, with damped magnitudes along with time, and approximately disappear at 2 hr. Since the vortex spindown is mainly resulted from imbalanced mass and wind fields at the initial time, the vortex can reintensify after the imbalance is damped by the spurious gravity wave through the geostrophic adjustment. Thus, given the time scale of spindown (∼1 hr), the gravity wave just propagates from the vortex center to the outside of the vortex. Compared to experiment CTRL, experiment 3DIAU does not obviously suffer the imbalance with gravity waves. During the 2 hr, experiment 3DIAU always has less pressure tendency than experiment CTRL. Since experiments with IAU have better vortex intensity and structure than experiment CTRL, the advantages of having a more balanced assimilation and more effective ingestion of observation information for IAU are proved.

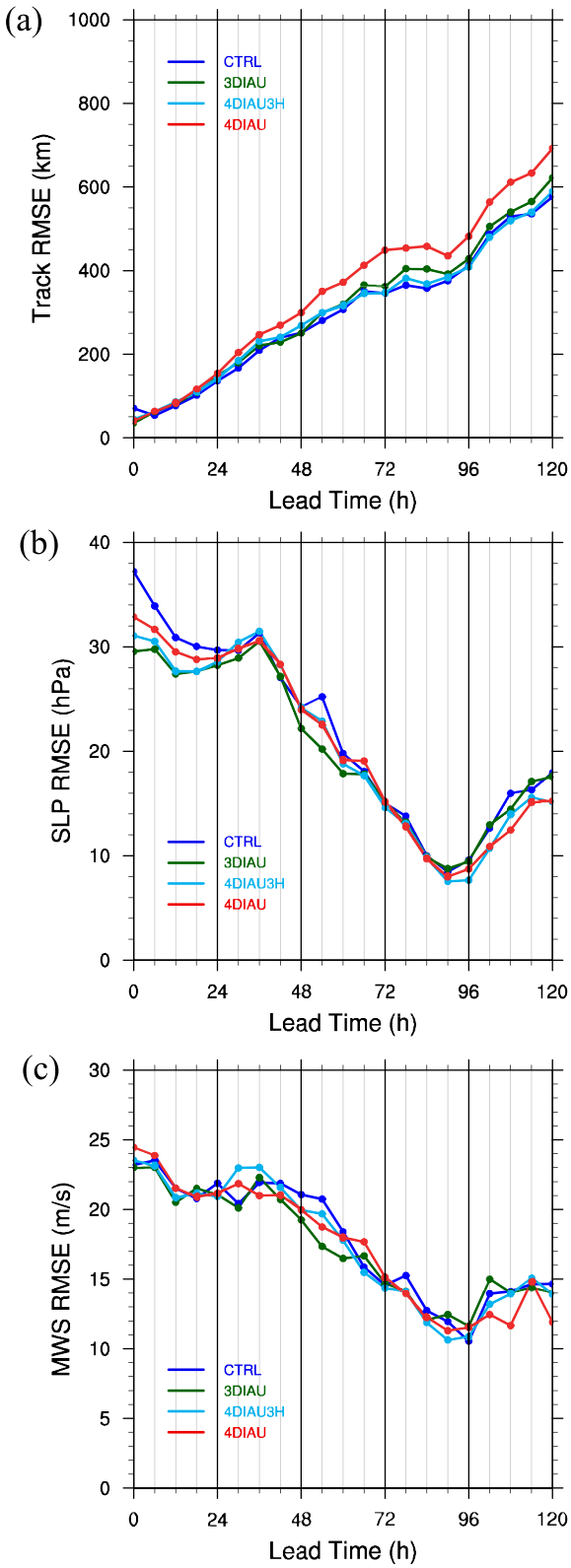

Figure 8. Root-mean-square errors (RMSEs) of (a) track, (b) minimum sea level pressure (SLP), and (c) maximal wind speed (MWS) as a function of forecast lead time initialized every 12 hr from the cycle experiments of typhoons Hagibis and Lingling.

4.3. Benefits of 3DIAU Over 4DIAU in the TC Intensity

Intuitively, 4DIAU can be more beneficial for the assimilation and forecast of TC than 3DIAU, since during an assimilation window 4DIAU can consider the temporal propagation of analysis increment, while 3DIAU has a constant analysis increment. But experiment 4DIAU shows a slightly weaker vortex than experiment 3DIAU (Figure 9). Lu and Wang (2021) found that the predetermined analysis increments can be detrimental for the incremental update and subsequent forecast, when there are discrepancies between the priors and posteriors during a nonlinear evolution. To investigate the impacts on vortex evolution from different implementations of IAU, hourly simulations and increments of u- and v-wind components at the lowest model level from the single-cycle experiments for experiments with IAU are examined. Figure 13 shows the simulations and increments in a $5° \times 5°$ box centered around the observed vortex during the assimilation window. To examine the cumulative effects of various IAU, the mean of hourly simulations and increments with vortex centered in the domain is also computed (rightmost columns).

The increment applied by experiment 3DIAU is the one valid at the analysis time 0 hr and is held constant through the assimilation window. Before the simulated vortex moves to the observed vortex at 0 hr and after the simulated vortex moves away from the observed vortex, the applied increment by 3DIAU and the simulated vortex have mismatches. The imposition of the temporal mismatched increment by 3DIAU may result in unrealistic evolution of a vortex or even cause detrimental effect for a fast moving/developing vortex.

Experiment 4DIAU (4DIAU3H) utilizes hourly (3-hr) increments that are interpolated to every model time step during the assimilation window. Thus, the increments at −3, 0, and 3 hr for experiments 4DIAU and 4DIAU3H are the same. Due to coarser temporal-resolution increments of 4DIAU3H than 4DIAU, model simulations from experiments 4DIAU and 4DIAU3H are slightly different. Compared to the increment of experiment 3DIAU, the increments of experiments 4DIAU and 4DIAU3H propagate within the assimilation window, which are resulted from more frequent background fields and associated sample background error covariances, and also unevenly temporal-distributed observations in an assimilation window. Also compared to 3DIAU, experiments 4DIAU and 4DIAU3H have increments aligning with the vortex at each time when an analysis is available. Since the simulated vortex locates northeast of the observed one, the increments within the assimilation window persistently suggest moving the simulated vortex to the south, which are shown by a cyclonic circulation at the south of the vortex from −3 to 3 hr. Because of different vortex centers resulted from simulations and observations, the increments by 4DIAU and 4DIAU3H tend to build a vortex around the observed vortex location rather than intensify the vortex at the simulated vortex center. Especially from 1 to 3 hr, the increments of experiment 4DIAU impose significantly negative u-wind extend to the west of the vortex center and negative v-wind along the west of the vortex center, which lead to a weakened vortex as shown in Figure 9.

The cumulative effects from different IAU experiments at the end of the assimilation window show that all three IAU experiments have an anticyclonic circulation to the north of the simulated vortex center and a cyclonic circulation to the south of the simulated vortex because of the mismatched vortex centers between the simulation and observation. Experiment 3DIAU has smoother mean increment than the two 4DIAU experiments. Due to the

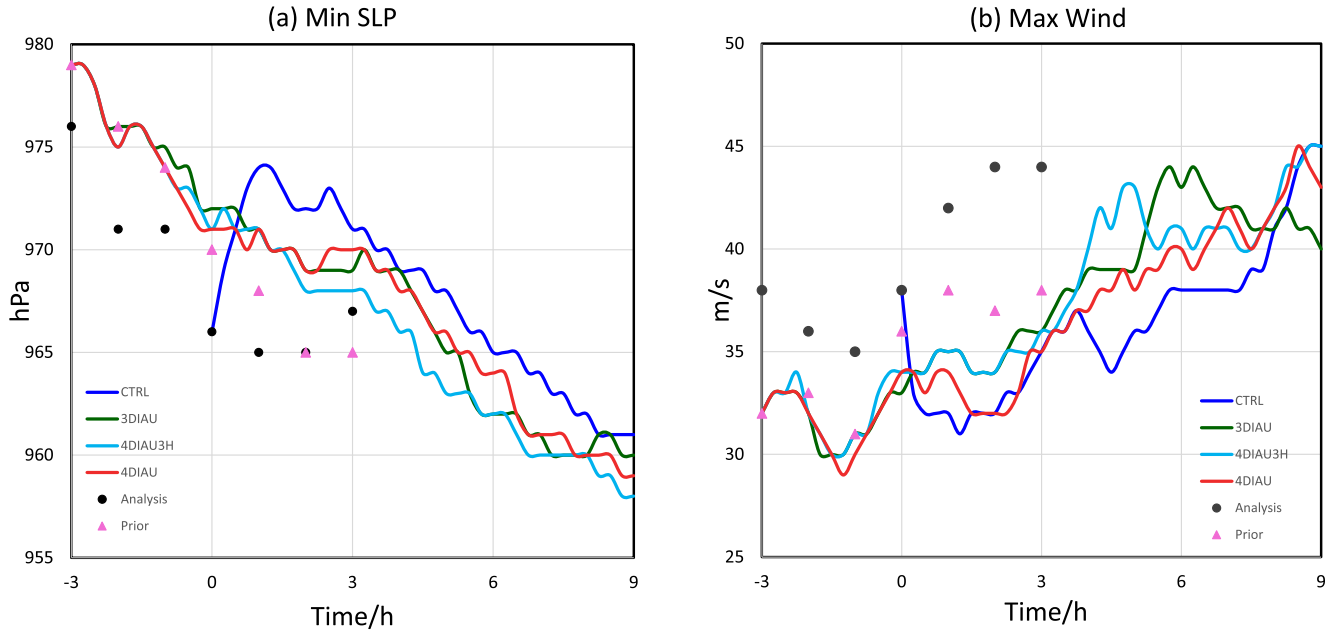

Figure 9. Evolution of minimum sea level pressure (SLP) and maximal wind speed (MWS) at the lowest model level during a 6-hr assimilation window centered at 1800 UTC 7 October 2019 and the adjacent next assimilation window. Please note that observed values for the minimum SLP and 10-m MWS at 1800 UTC 7 October 2019 (0 hr) are 915 hPa and 71 m/s.

temporal mismatch of increments, the vortex adjustment (movement or intensification) suggested by the observations has been neglected in experiment 3DIAU. Compared to experiment 3DIAU, experiments 4DIAU and 4DIAU3H consider the propagation of increment during the assimilation window and act as a weaker filter, and then the mean increments of experiments 4DIAU and 4DIAU3H contain more fine structures. But due to the vortex position error, experiment 4DIAU imposes a stronger anticyclonic circulation around the simulated vortex center than experiment 4DIAU3H, and hence, experiment 4DIAU results in a more weakened vortex than experiment 4DIAU3H. Thus for TC, the advantage of 4DIAU that considers temporal propagation of increment during the analysis window is limited by the analysis increment with mismatch of vortex center from the simulation and observation. 4DIAU3H takes a trade-off between 4DIAU and 3DIAU, since it uses less frequent analysis increments than 4DIAU but considers time-varying increments compared to 3DIAU.

From 3DIAU to 4DIAU3H and then to 4DIAU, the filtering effect decreases, while the temporal resolution of the analysis-increment propagation within an assimilation window increases. The high-frequency components of the time-varying analysis increments can be contaminated by sampling errors and model errors (Lei & Whitaker, 2016). They can also be affected by the position errors of moving weather systems (Figure 13). Although Lei and Whitaker (2016) showed that increasing the frequency of analysis increments could improve the performance of 4DIAU, the position error of the simulated vortex in WRF results in spurious high-frequency components of the analysis increment. Thus, the advantages of 4DIAU with higher-frequency analysis increment are limited, and an intermittent 4DIAU3H is preferred for the vortex cases. The vortex simulated could be further improved by 4DIAU with higher-frequency components of the analysis increments that can realistically capture the evolution of vortex, which can be achieved by relocating the simulated vortex to the observed location or computing feature-relative increments (Lu & Wang, 2021).

5. Discussions and Conclusions

Different implementations of IAU with time-constant increments or time-varying increments constructed using different frequencies of analysis increment are systematically evaluated in the regional model WRF for two case studies of fast-evolving typhoons. Verifications against the conventional observations and NCEP FNL analyses show that experiments with IAU generally produce smaller errors of temperature, specific humidity, and wind speed than experiment CTRL that has no initialization applied. Experiment 3DIAU has significantly smaller errors than 4DIAU3H, and 4DIAU3H generally has significantly smaller errors than 4DIAU. Consistently, exper-

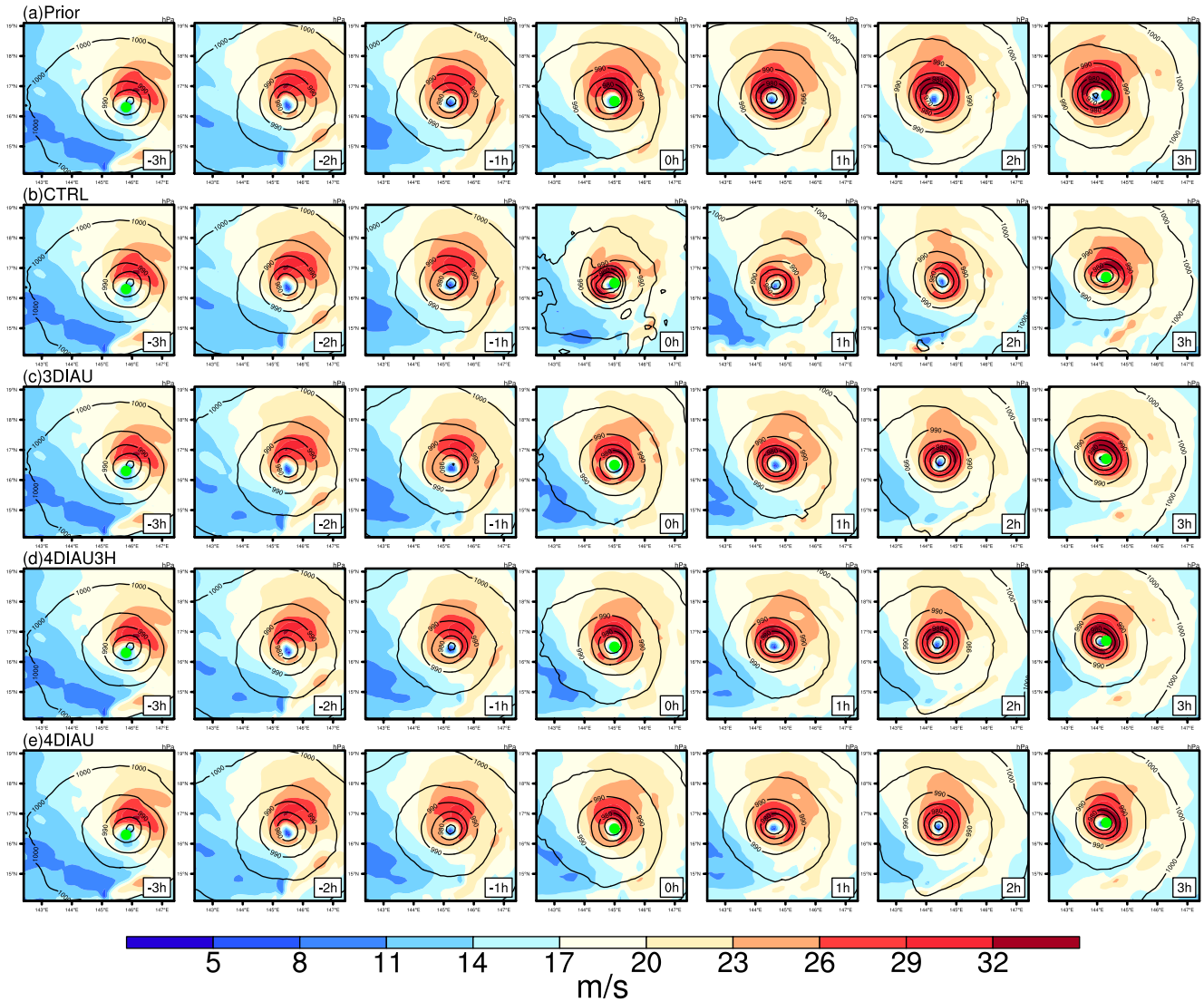

Figure 10. Hourly evolution of the wind speed at the lowest model level (m/s; shading) and sea level pressure (hPa; contours) for assimilation window centered at 1800 UTC 7 October 2019 (−3 to 3 hr of Figure 9) for (a) free forecast, (b) CTRL, (c) three-dimensional incremental analysis update (3DIAU), (d) four-dimensional incremental analysis update with 3-hr analysis increments (4DIAU3H), and (e) four-dimensional incremental analysis update (4DIAU). Green dots denote the interpolated 3-hr tropical cyclone (TC) locations using Tropical Cyclone Vitals Database.

iments with IAU have significantly smaller magnitudes of surface pressure tendency than experiment CTRL. Experiment 3DIAU has significantly smaller magnitudes of surface pressure tendency than 4DIAU3H, and experiment 4DIAU3H has significantly smaller magnitudes of surface pressure tendency than 4DIAU. Thus, for the regional WRF model, 3DIAU that imposes stronger filtering, that is, more effective reduction of imbalance in intermittent DA, has advantages over 4DIAU with different frequencies of analysis increment. These findings are different from Lei and Whitaker (2016) based on the NCEP GFS model. The inconsistent results may relate with different models, since the regional model WRF has higher spatial resolutions and may prefer stronger filtering for the unbalanced analysis increments than the global model GFS. The degree of damping and associated impacts on IAU in different models will be further investigated.

For two typhoon cases, experiments with IAU obtain better intensity and structure of the vortex than experiment CTRL. Experiments with IAU have significantly smaller errors of TC fullness, which are an integrated measurement of the TC outer-core and inner-core structures, than experiment CTRL with the advantages mainly led by the improvement of RMW. Moreover, the application of IAU is beneficial for developing coherent TC structures at early stages. The analyses of high-frequent evolutions of pressure, wind, and dry air mass tendency show that the vortex spindown

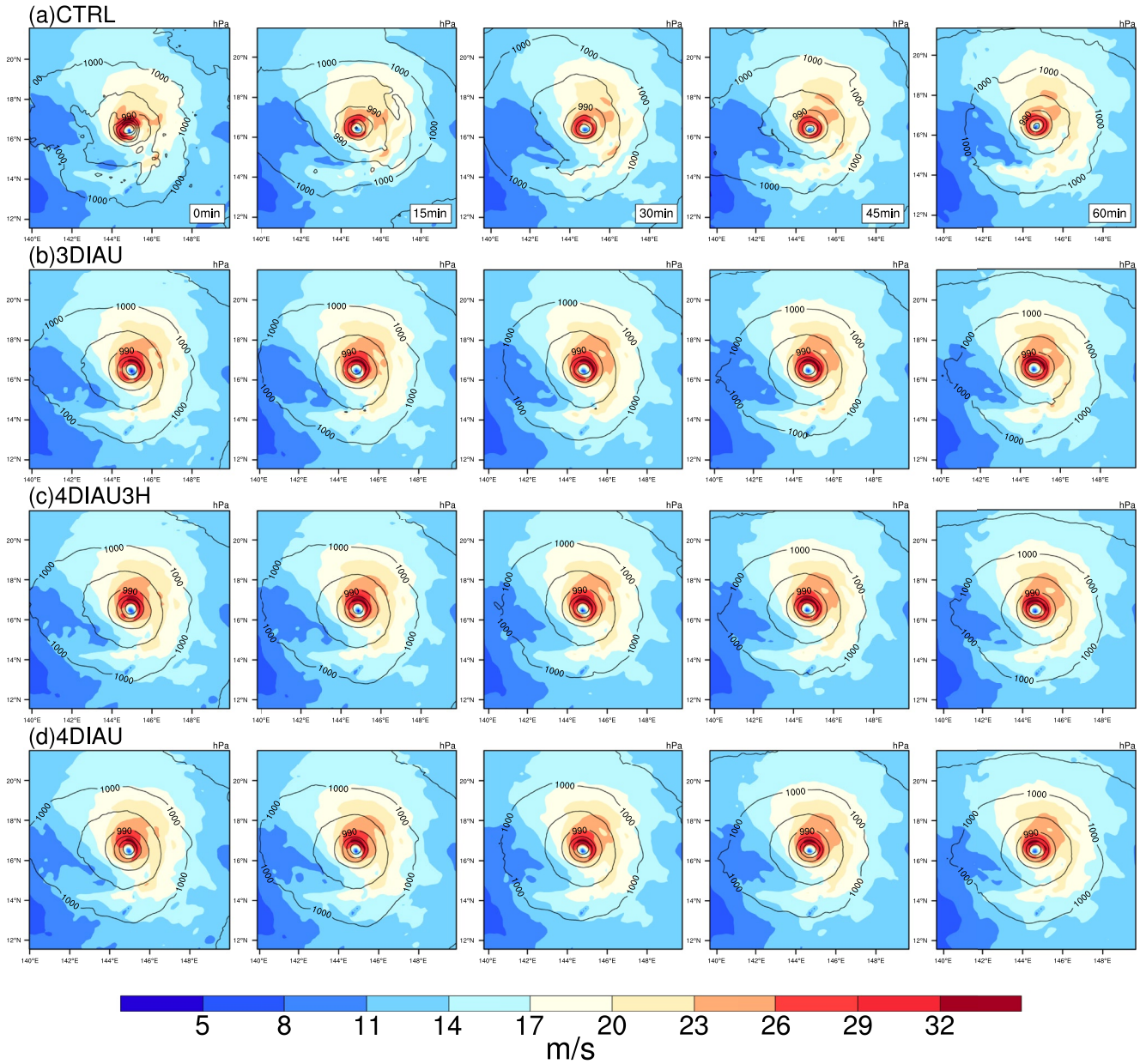

Figure 11. A 15-min evolution of wind speed at the lowest model level (m/s; shading) and sea level pressure (hPa; contours) from 1800 UTC to 1900 UTC 7 October 2019 (0–1 hr of Figure 9) for experiments (a) CTRL, (b) three-dimensional incremental analysis update (3DIAU), (c) four-dimensional incremental analysis update with 3-hr analysis increments (4DIAU3H), and (d) four-dimensional incremental analysis update (4DIAU).

and rapid adjustment due to unbalanced increments are mitigated by the application of IAU. Thus, experiments with IAU can better retain the observation information and build the improved TC structure during its evolution.

Compared to 3DIAU, 4DIAU considers the propagation of increment and contains more increment structures during an assimilation window. But due to the analysis increment with mismatch of vortex center from the simulation and observation, the advantage of 4DIAU over 3DIAU is limited, since 4DIAU does not improve the TC intensity compared to 3DIAU. As a trade-off between the filtering and time-varying increment, 4DIAU3H that uses less frequent analysis increments than 4DIAU but considers time-varying increments compared to 3DIAU is preferred. As shown by Lu and Wang (2021), vortex relocation or feature-relative approach can remedy the limitation of predetermined analysis increments with discrepancies between the priors and posteriors for 4DIAU. But these methods introduce additional steps for the analysis increments and also relied on feature processing.

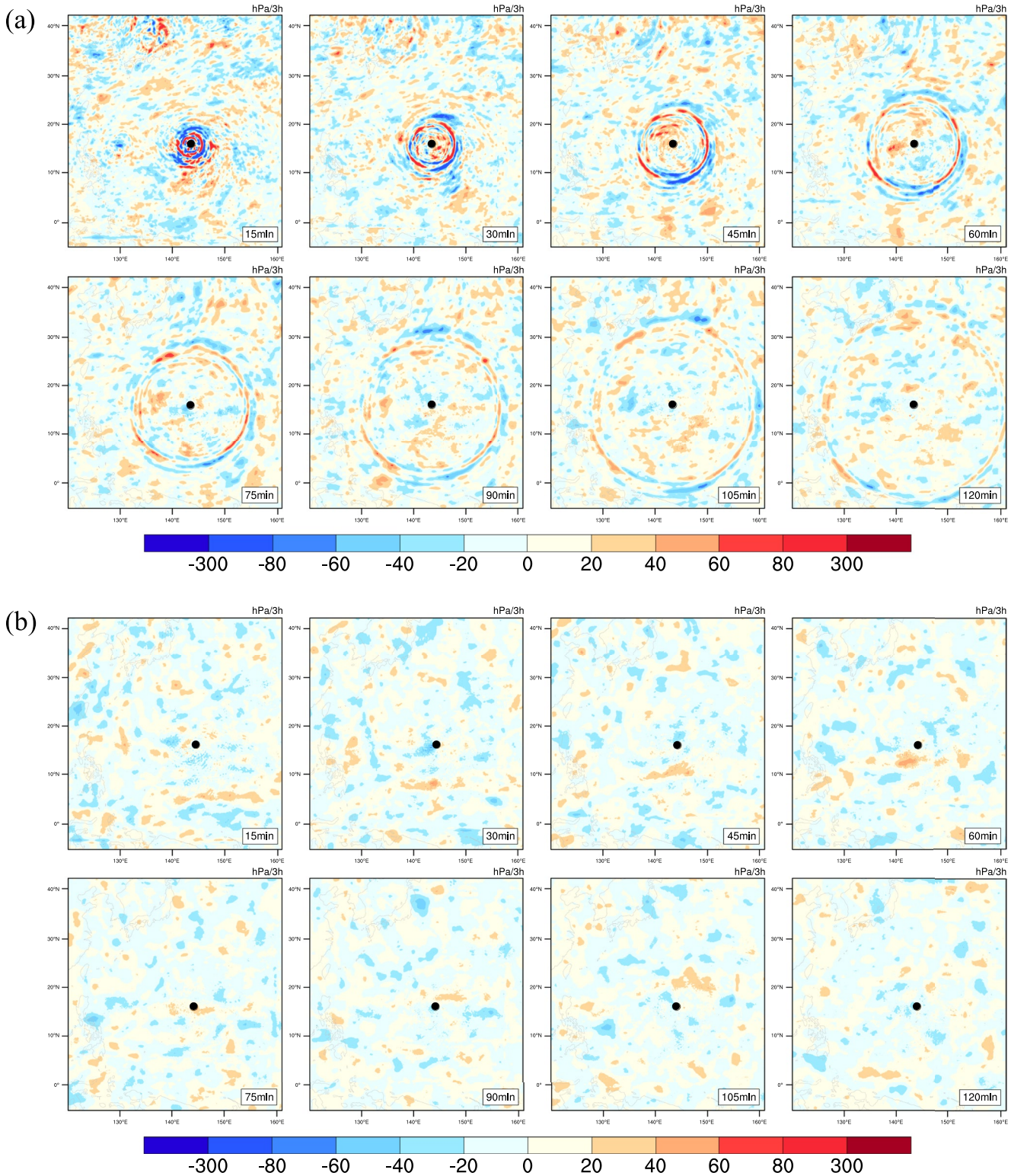

Figure 12. A 15-min evolution of the dry air mass tendency (hPa/3h) from 1800 UTC to 2000 UTC 7 October 2019 (0–2 hr of Figure 9) for experiments (a) CTRL and (b) three-dimensional incremental analysis update. The black dots denote the tropical cyclone position at 1800 UTC.

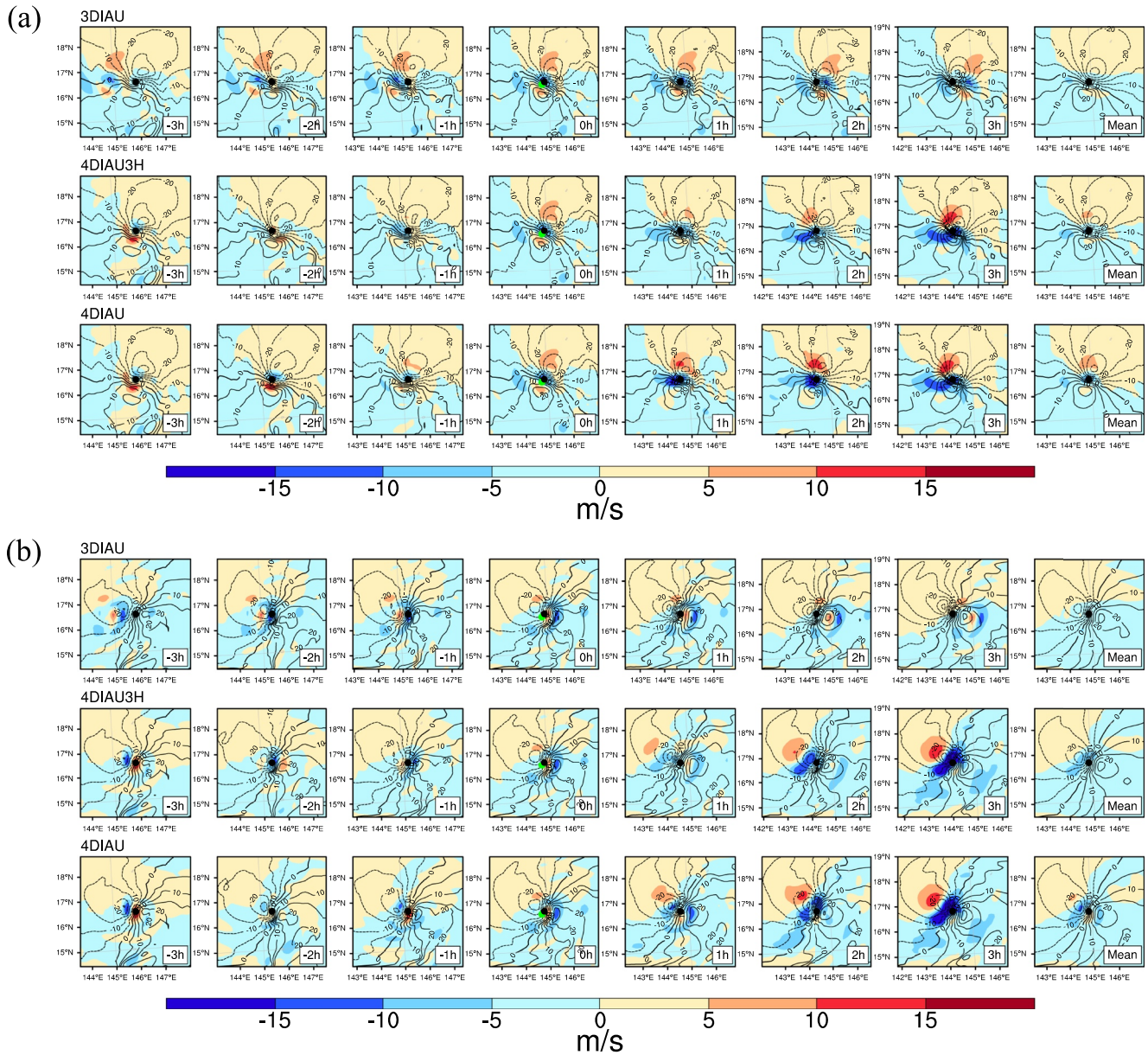

Figure 13. Simulations (contours) and increments (shading) for (a) u-wind and (b) v-wind components at the lowest model level from the 6-hr assimilation window centered at 1800 UTC 7 October 2019. In each subplot, upper, middle, and lower panels show experiments three-dimensional incremental analysis update (3DIAU), four-dimensional incremental analysis update with 3-hr analysis increments (4DIAU3H), and four-dimensional incremental analysis update (4DIAU), respectively, and the rightmost column displays the mean from −3 to 3 hr. Black and green dots denote the tropical cyclone center from simulations and observations, respectively.

The nonlinear evolution of analysis increments might be mitigated by high-frequent update, which will be further investigated. Impacts of IAU on fast-moving systems, like the mesoscale convective systems, also need further studies. Moreover, the performances of IAU with fine resolutions (e.g., convective-scale simulations at O(1 km)) and moving nested domains will be examined in a future study.

Data Availability Statement

To generate the data assimilation (DA) experiments, the meteorological data used for the initial conditions at the beginning of the experiment and boundary conditions are obtained from the National Centers for Environmental Prediction Global Forecast System (NCEP GFS; https://www.ncei.noaa.gov/products/weather-climate-models/global-forecast), and the assimilated observations are obtained from the NCEP Global Data Assimilation System

(https://www.ncei.noaa.gov/products/weather-climate-models/global-data-assimilation). The Weather Research and Forecasting model version 3.9 is available at https://www.mmm.ucar.edu/weather-research-and-forecasting-model and the Gridpoint Statistical Interpolation/ensemble Kalman filter is available at https://dtcenter.org/community-code/gridpoint-statistical-interpolation-gsi. The results of the DA experiments are available at https://meso.nju.edu.cn/xwdt/20220711/i225901.html.

Acknowledgments
The authors thank the three anonymous reviewers for their insightful and constructive comments and suggestions. This work was supported by the National Key Research and Development Program of China under Grant 2017YFC1501603, the National Natural Science Foundation of China under Grants 41922036 and 42192553, the Frontiers Science Center for Critical Earth Material Cycling Fund JBGS2102, and the Fundamental Research Funds for the Central Universities 0209-14380097.

References

Baer, F., & Tribbia, J. J. (1977). On complete filtering of gravity modes through nonlinear initialization. *Monthly Weather Review*, *105*(12), 1536–1539. https://doi.org/10.1175/1520-0493(1977)105<1536:OCFOGM>2.0.CO;2

Benkiran, M., & Greiner, E. (2008). Impact of the incremental analysis updates on a real-time system of the North Atlantic Ocean. *Journal of Atmospheric and Oceanic Technology*, *25*(11), 2055–2073. https://doi.org/10.1175/2008JTECHO537.1

Bergemann, K., & Reich, S. (2010). A mollified ensemble Kalman filter. *Quarterly Journal of the Royal Meteorological Society*, *136*(651), 1636–1643. https://doi.org/10.1002/qj.672

Bloom, S. C., Takacs, L. L., Da Silva, A. M., & Ledvina, D. (1996). Data assimilation using incremental analysis updates. *Monthly Weather Review*, *124*(6), 1256–1271. https://doi.org/10.1175/1520-0493(1996)124<1256:DAUIAU>2.0.CO;2

Buehner, M., McTaggart-Cowan, R., Beaulne, A., Charette, C., Garand, L., Heilliette, S., et al. (2015). Implementation of deterministic weather forecasting systems based on ensemble-variational data assimilation at Environment Canada. Part I: The global system. *Monthly Weather Review*, *143*(7), 2532–2559. https://doi.org/10.1175/MWR-D-14-00354.1

Buehner, M., Morneau, J., & Charette, C. (2013). Four-dimensional ensemble-variational data assimilation for global deterministic weather prediction. *Nonlinear Processes in Geophysics*, *20*(5), 669–682. https://doi.org/10.5194/npg-20-669-2013

Carton, J. A., Chepurin, G., Cao, X., & Giese, B. (2000). A simple ocean data assimilation analysis of the global upper ocean 1950–95. Part I: Methodology. *Journal of Physical Oceanography*, *30*(2), 294–309. https://doi.org/10.1175/1520-0485(2000)030<0294:ASODAA>2.0.CO;2

Clayton, A. M., Lorenc, A. C., & Barker, D. M. (2013). Operational implementation of a hybrid ensemble/4D-VAR global data assimilation system at the Met Office. *Quarterly Journal of the Royal Meteorological Society*, *139*(675), 1445–1461. https://doi.org/10.1002/qj.2054

Evensen, G. (1994). Sequential data assimilation with a nonlinear quasi-geostrophic model using Monte Carlo methods to forecast error statistics. *Journal of Geophysical Research*, *99*(C5), 10143–10162. https://doi.org/10.1029/94JC00572

Feng, J., & Wang, X. (2021). Impact of increasing horizontal and vertical resolution of the hurricane WRF model on the analysis and prediction of Hurricane Patricia (2015). *Monthly Weather Review*, *149*(2), 419–441. https://doi.org/10.1175/MWR-D-20-0144.1

Fujita, T., Stensrud, D. J., & Dowell, D. C. (2007). Surface data assimilation using an ensemble Kalman filter approach with initial condition and model physics uncertainties. *Monthly Weather Review*, *135*(5), 1846–1868. https://doi.org/10.1175/MWR3391.1

Gaspari, G., & Cohn, S. E. (1999). Construction of correlation functions in two and three dimensions. *Quarterly Journal of the Royal Meteorological Society*, *125*(554), 723–757. https://doi.org/10.1002/qj.49712555417

Guo, X., & Tan, Z.-M. (2017). Tropical cyclone fullness: A new concept for interpreting storm intensity. *Geophysical Research Letters*, *44*(9), 4324–4331. https://doi.org/10.1002/2017GL073680

Ha, S., Snyder, C., Skamarock, W. C., Anderson, J., & Collins, N. (2017). Ensemble Kalman filter data assimilation for the model for prediction across scales (MPAS). *Monthly Weather Review*, *145*(11), 4673–4692. https://doi.org/10.1175/MWR-D-17-0145.1

Hamill, T. M., & Snyder, C. (2000). A hybrid ensemble Kalman filter-3D variational analysis scheme. *Monthly Weather Review*, *128*(8 II), 2905–2919. https://doi.org/10.1175/1520-0493(2000)128<2905:ahekfv>2.0.co;2

Harms, D. E., Raman, S., & Madala, R. V. (1992). An examination of four-dimensional data-assimilation techniques for numerical weather prediction. *Bulletin of the American Meteorological Society*, *73*(4), 425–440. https://doi.org/10.1175/1520-0477(1992)073<0425:AEOFDD>2.0.CO;2

He, H., Lei, L., Whitaker, J. S., & Tan, Z. M. (2020). Impacts of assimilation frequency on ensemble Kalman filter data assimilation and imbalances. *Journal of Advances in Modeling Earth Systems*, *12*(10), e2020MS002187. https://doi.org/10.1029/2020MS002187

Hendricks, E. A., Peng, M. S., Ge, X., & Li, T. (2011). Performance of a dynamic initialization scheme in the Coupled Ocean–Atmosphere Mesoscale Prediction System for Tropical Cyclones (COAMPS-TC). *Weather and Forecasting*, *26*(5), 650–663. https://doi.org/10.1175/WAF-D-10-05051.1

Hong, S. Y., & Lim, J. O. J. (2006). The WRF single-moment 6-class micro physics scheme (WSM6). *Journal of the Korean Meteorological Society*, *42*, 129–151.

Hong, S. Y., Noh, Y., & Dudhia, J. (2006). A new vertical diffusion package with an explicit treatment of entrainment processes. *Monthly Weather Review*, *134*(9), 2318–2341. https://doi.org/10.1175/MWR3199.1

Huang, X.-Y., & Lynch, P. (1993). Diabatic digital-filtering initialization: Application to the HIRLAM model. *Monthly Weather Review*, *121*(2), 589–603. https://doi.org/10.1175/1520-0493(1993)121<0589:DDFIAT>2.0.CO;2

Hunt, B. R., Kalnay, E., Kostelich, E. J., Ott, E., Patil, D. J., Sauer, T., et al. (2004). Four-dimensional ensemble Kalman filtering. *Tellus A: Dynamic Meteorology and Oceanography*, *56*(4), 273–277. https://doi.org/10.1111/j.1600-0870.2004.00066.x

Iacono, M. J., Delamere, J. S., Mlawer, E. J., Shephard, M. W., Clough, S. A., & Collins, W. D. (2008). Radiative forcing by long–lived greenhouse gases: Calculations with the AER radiative transfer models. *Journal of Geophysical Research*, *113*(D13), D13103. https://doi.org/10.1029/2008JD009944

Islam, T., Srivastava, P. K., Rico-Ramirez, M. A., Dai, Q., Gupta, M., & Singh, S. K. (2015). Tracking a tropical cyclone through WRF–ARW simulation and sensitivity of model physics. *Natural Hazards*, *76*(3), 1473–1495. https://doi.org/10.1007/s11069-014-1494-8

Kain, J. S. (2004). The Kain–Fritsch convective parameterization: An update. *Journal of Applied Meteorology*, *43*(1), 170–181. https://doi.org/10.1175/1520-0450(2004)043<0170:TKCPAU>2.0.CO;2

Kleist, D. T., & Ide, K. (2015a). An OSSE-based evaluation of hybrid variational–ensemble data assimilation for the NCEP GFS. Part I: System description and 3D-hybrid results. *Monthly Weather Review*, *143*(2), 433–451. https://doi.org/10.1175/MWR-D-13-00351.1

Kleist, D. T., & Ide, K. (2015b). An OSSE-based evaluation of hybrid variational–ensemble data assimilation for the NCEP GFS. Part II: 4DEnVar and hybrid variants. *Monthly Weather Review*, *143*(2), 452–470. https://doi.org/10.1175/MWR-D-13-00350.1

Kleist, D. T., Parrish, D. F., Derber, J. C., Treadon, R., Wu, W. S., & Lord, S. (2009). Introduction of the GSI into the NCEP global data assimilation system. *Weather and Forecasting*, *24*(6), 1691–1705. https://doi.org/10.1175/2009WAF2222201.1

Kuhl, D. D., Rosmond, T. E., Bishop, C. H., McLay, J., & Baker, N. L. (2013). Comparison of hybrid ensemble/4DVar and 4DVar within the NAVDAS-AR data assimilation Framework. *Monthly Weather Review*, *141*(8), 2740–2758. https://doi.org/10.1175/MWR-D-12-00182.1

Lei, L., Stauffer, D. R., & Deng, A. (2012a). A hybrid nudging-ensemble Kalman filter approach to data assimilation. Part II: Application in a shallow-water model. *Tellus A: Dynamic Meteorology and Oceanography*, *64A*(1), 18485. https://doi.org/10.3402/tellusa.v64i0.18485

Lei, L., Stauffer, D. R., & Deng, A. (2012b). A hybrid nudging-ensemble Kalman filter approach to data assimilation in WRF/DART. *Quarterly Journal of the Royal Meteorological Society*, *138*(669), 2066–2078. https://doi.org/10.1002/qj.1939

Lei, L., Stauffer, D. R., Haupt, S. E., & Young, G. S. (2012). A hybrid nudging-ensemble Kalman filter approach to data assimilation. Part I: Application in the Lorenz system. *Tellus A: Dynamic Meteorology and Oceanography*, *64A*(1), 18484. https://doi.org/10.3402/tellusa.v64i0.18484

Lei, L., & Whitaker, J. S. (2016). A four-dimensional incremental analysis update for the ensemble Kalman filter. *Monthly Weather Review*, *144*(7), 2605–2621. https://doi.org/10.1175/MWR-D-15-0246.1

Liu, C., & Xiao, Q. (2013). An ensemble-based four-dimensional variational data assimilation scheme. Part III: Antarctic applications with advanced research WRF using real data. *Monthly Weather Review*, *141*(8), 2721–2739. https://doi.org/10.1175/MWR-D-12-00130.1

Liu, C., Xiao, Q., & Wang, B. (2009). An ensemble-based four-dimensional variational data assimilation scheme. Part II: Observing system simulation experiments with advanced research WRF (ARW). *Monthly Weather Review*, *137*(5), 1687–1704. https://doi.org/10.1175/2008MWR2699.1

Lorenc, A. C. (2003). The potential of the ensemble Kalman filter for NWP – A comparison with 4D-var. *Quarterly Journal of the Royal Meteorological Society*, *129*(595 PART B), 3183–3203. https://doi.org/10.1256/qj.02.132

Lorenc, A. C., Bowler, N. E., Clayton, A. M., Pring, S. R., & Fairbairn, D. (2015). Comparison of hybrid-4DEnVar and hybrid-4DVar data assimilation methods for global NWP. *Monthly Weather Review*, *143*(1), 212–229. https://doi.org/10.1175/MWR-D-14-00195.1

Lu, X., & Wang, X. (2019). Improving Hurricane analyses and predictions with TCI, IFEX field campaign observations, and CIMSS AMVs using the advanced hybrid data assimilation system for HWRF. Part I: What is missing to capture the rapid intensification of Hurricane Patricia (2015). *Monthly Weather Review*, *147*(4), 1351–1373. https://doi.org/10.1175/MWR-D-18-0202.1

Lu, X., & Wang, X. (2021). Improving the four-dimensional incremental analysis update (4DIAU) with the HWRF 4DEnVar data assimilation system for rapidly evolving hurricane prediction. *Monthly Weather Review*, *149*(12), 4027–4043. https://doi.org/10.1175/MWR-D-21-0068.1

Lynch, P., & Huang, X.-Y. (1992). Initialization of the HIRLAM model using a digital filter. *Monthly Weather Review*, *120*(6), 1019–1034. https://doi.org/10.1175/1520-0493(1992)120<1019:IOTHMU>2.0.CO;2

Machenhauer, B. (1977). On the dynamics of gravity oscillations in a shallow water model, with applications to normal mode initialization. *Beitrage zur Physik der Atmosphare*, *50*(1), 253–271.

Ourmières, Y., Brankart, J. M., Berline, L., Brasseur, P., & Verron, J. (2006). Incremental analysis update implementation into a sequential ocean data assimilation system. *Journal of Atmospheric and Oceanic Technology*, *23*(12), 1729–1744. https://doi.org/10.1175/JTECH1947.1

Polavarapu, S., Ren, S., Clayton, A. M., Sankey, D., & Rochon, Y. (2004). On the relationship between incremental analysis updating and incremental digital filtering. *Monthly Weather Review*, *132*(10), 2495–2502. https://doi.org/10.1175/1520-0493(2004)132<2495:otrbia>2.0.co;2

Ren, S., Lei, L., Tan, Z.-M., & Zhang, Y. (2019). Multivariate ensemble sensitivity analysis for super typhoon Haiyan (2013). *Monthly Weather Review*, *147*(9), 3467–3480. https://doi.org/10.1175/MWR-D-19-0074.1

Rienecker, M. M., Suarez, M. J., Todling, R., Bacmeister, J., Takacs, L., Liu, H.-C., et al. (2008). The GEOS-5 data assimilation system: Documentation of versions 5.0.1 and 5.1.0, and 5.2.0 (NASA Tech. Rep. Series on Global Modeling and Data Assimilation, NASA/TM-2008–104606, Vol. *27*, pp. 92). NASA Goddard Space Flight Center.

Sawada, M., Ma, Z., Mehra, A., Tallapragada, V., Oyama, R., & Shimoji, K. (2019). Impacts of assimilating high-resolution atmospheric motion vectors derived from Himawari-8 on tropical cyclone forecast in HWRF. *Monthly Weather Review*, *147*(10), 3721–3740. https://doi.org/10.1175/MWR-D-18-0261.1

Schwartz, C. S., Poterjoy, J., Carley, J. R., Dowell, D. C., Romine, G. S., & Ide, K. (2021). Comparing partial and continuously cycling ensemble Kalman filter data assimilation systems for convection-allowing ensemble forecast initialization. *Weather and Forecasting*, *37*(1), 85–112. https://doi.org/10.1175/WAF-D-21-0069.1

Skamarock, W. C., Klemp, J. B., Dudhia, J., Gill, D. O., Barker, D. M., Duda, M. G., et al. (2008). *A description of the advanced research WRF Version 3* (NCAR Tech Note NCAR/TN-475 + STR). NCAR. https://doi.org/10.5065/D68S4MVH

Stauffer, D. R., & Seaman, N. L. (1990). Use of four-dimensional data assimilation in a limited-Area mesoscale model. Part I: Experiments with synoptic-scale data. *Monthly Weather Review*, *118*(6), 1250–1277. https://doi.org/10.1175/1520-0493(1990)118<1250:UOFDDA>2.0.CO;2

Stauffer, D. R., & Seaman, N. L. (1994). Multiscale four-dimensional data assimilation. *Journal of Applied Meteorology and Climatology*, *33*(3), 416–434. https://doi.org/10.1175/1520-0450(1994)033<0416:MFDDA>2.0.CO;2

Takacs, L., Suarez, M. J., & Todling, R. (2018). The stability of incremental analysis update. *Monthly Weather Review*, *146*(10), 3259–3275. https://doi.org/10.1175/MWR-D-18-0117.1

Tewari, M., Chen, F., Wang, W., Dudhia, J., LeMone, M. A., Mitchell, K., et al. (2004). Implementation and verification of the unified NOAH land surface model in the WRF model. *Paper presented at 20th Conference on Weather Analysis and Forecasting/16th Conference on Numerical Weather Prediction, Seattle*.

Tong, M., Sippel, J. A., Tallapragada, V., Liu, E., Kieu, C., Kwon, I., et al. (2018). Impact of assimilating aircraft reconnaissance Observations on tropical cyclone initialization and prediction using Operational HWRF and GSI ensemble – Variational hybrid data assimilation. *Monthly Weather Review*, *146*(12), 4155–4177. https://doi.org/10.1175/MWR-D-17-0380.1

Vukicevic, T., Aksoy, A., Reasor, P., Aberson, S. D., Sellwood, K. J., & Marks, F. (2013). Joint impact of forecast tendency and state error biases in ensemble Kalman filter data assimilation of inner-core tropical cyclone observations. *Monthly Weather Review*, *141*(9), 2992–3006. https://doi.org/10.1175/MWR-D-12-00211.1

Wang, C., Lei, L., Tan, Z.-M., & Chu, K. (2020). Adaptive localization for tropical cyclones with satellite radiances in an ensemble Kalman filter. *Frontiers of Earth Science*, *8*(39), 1–16. https://doi.org/10.3389/feart.2020.00039

Wang, X., Barker, D. M., Snyder, C., & Hamill, T. M. (2008). A hybrid ETKF–3DVAR data assimilation scheme for the WRF model. Part II: Real observation experiments. *Monthly Weather Review*, *136*(12), 5132–5147. https://doi.org/10.1175/2008MWR2445.1

Whitaker, J. S., & Hamill, T. M. (2002). Ensemble data assimilation without perturbed observations. *Monthly Weather Review*, *130*(7), 1913–1924. https://doi.org/10.1175/1520-0493(2002)130<1913:EDAWPO>2.0.CO;2

Whitaker, J. S., & Hamill, T. M. (2012). Evaluating methods to account for system errors in ensemble data assimilation. *Monthly Weather Review*, *140*(9), 3078–3089. https://doi.org/10.1175/MWR-D-11-00276.1

Wu, W., Purser, R. J., & Parrish, D. F. (2002). Three-dimensional variational analysis with spatially inhomogeneous covariances. *Monthly Weather Review*, *130*(12), 2905–2916. https://doi.org/10.1175/1520-0493(2002)130<2905:TDVAWS>2.0.CO;2

Zeng, Y., de Lozar, A., Janjic, T., & Seifert, A. (2021). Applying a new integrated mass-flux adjustment filter in rapid update cycling of convective-scale data assimilation for the COSMO-model (v5.07). *Geoscientific Model Development*, *14*(3), 1295–1307. https://doi.org/10.5194/gmd-2020-299

Zhang, M., & Zhang, F. (2012). E4DVar: Coupling an ensemble Kalman filter with four-dimensional variational data assimilation in a limited-area weather prediction model. *Monthly Weather Review*, *140*(2), 587–600. https://doi.org/10.1175/MWR-D-11-00023.1

Zhu, Y., Todling, R., Guo, J., Cohn, S. E., Navon, I. M., & Yang, Y. (2003). The GEOS-3 retrospective data assimilation system: The 6-hour lag case. *Monthly Weather Review*, *131*(9), 2129–2150. https://doi.org/10.1175/1520-0493(2003)131<2129:TGRDAS>2.0.CO;2